



High-Temperature Erosion of HVOF Sprayed $\text{Cr}_3\text{C}_2\text{-NiCr}$ Coating and Mild Steel for Boiler Tubes

Guan-Jun Yang, Chang-Jiu Li, Shi-Jun Zhang, and Cheng-Xin Li

(Submitted May 13, 2008; in revised form July 19, 2008)

The comparison of the high-temperature erosion behavior of a High-velocity oxyfuel (HVOF) sprayed $\text{Cr}_3\text{C}_2\text{-NiCr}$ coating with mild steel for circulating fluidized bed boiler tubes was investigated. Results showed that the erosion rate of the mild steel at 800 °C was four times that at 300 °C at an erosion angle of 30°. However, the erosion rate of the HVOF sprayed $\text{Cr}_3\text{C}_2\text{-NiCr}$ coating was not influenced by the temperature in the range of 300–800 °C. It was found that the erosion resistance of HVOF sprayed $\text{Cr}_3\text{C}_2\text{-NiCr}$ coating was more than three times higher than that of the mild steel at 700–800 °C. In addition to the ploughing on the coating surface, the cracking along splat interfaces in the coating was clearly observed on the cross-sectional microstructure. The results indicate that the erosion performance of the HVOF sprayed $\text{Cr}_3\text{C}_2\text{-NiCr}$ coating is controlled by the cohesion between splats and can be further enhanced by improving splat cohesion.

Keywords boiler tube, $\text{Cr}_3\text{C}_2\text{-NiCr}$ coating, high-temperature erosion, HVOF, mild steel

1. Introduction

Circulating fluidized bed (CFB) boilers are becoming more widely used in coal-fired power plants because of their advantages of high efficiency in the combustion of a wide variety of solid fuels, in-bed sulfur capture, and relatively low NO_x emission (Ref 1-3). The erosive wear resulting from the hard coal gangue is the main cause of failures in economizer boiler tubes at high temperature (Ref 2, 3). The improvement of the erosive wear resistance of the boiler tubes is therefore extremely important to elongate the continuous-operation time. The size of the coal gangue particles in CFB is on the millimeter scale, and the particle velocity is from several to tens of meters per second (Ref 4, 5). Remedial actions used to combat

the erosion wastage include design modifications, use of horizontal plates welded on the wall, and use of wear-resistant materials in the area at risk (Ref 6-8).

High-velocity oxyfuel (HVOF) sprayed $\text{Cr}_3\text{C}_2\text{-NiCr}$ coatings are one of the most important candidates for protection of materials from high-temperature wear and erosion and have been successfully used to protect pulverized coal-fired boiler tubes (Ref 6-8). Many papers investigate wear and erosion performance of HVOF sprayed $\text{Cr}_3\text{C}_2\text{-NiCr}$ and other cermet coatings (Ref 8-24). It was recognized that the erosion is much more complex than abrasive wear in which the wear resistance is predominantly influenced by the hardness of the coatings (Ref 15-24). The erosion behavior depends on the response behavior of coatings to the impact of erosive particles at high velocity (Ref 8-14). Microcutting, gouging, carbide peeling out, and splat flaking have been observed in the erosion of the HVOF sprayed $\text{Cr}_3\text{C}_2\text{-NiCr}$ coatings at room temperature (Ref 14). Microcutting and gouging can be partially understood from the viewpoint of abrasive wear. For example, since the wear resistance increases with the increase of carbide content and carbide hardness and the decrease of carbide size and carbon loss (Ref 17-22), the erosion resistance can also be improved by similar approaches (Ref 14). In addition, it is of interest to note that the erosion of the HVOF sprayed $\text{Cr}_3\text{C}_2\text{-NiCr}$ coatings at room temperature was significantly influenced by the spalling off of lamellae from the interlamellar interface (Ref 14). Furthermore, the wear resistance also depends on the powder feedstock characteristics. For instance, the wear resistance of the coating deposited with sinter-crushed powder was much higher than that with a blended powder of alloy powder and carbide powder in the work of Ref 24. This is because the coating deposited with the blended powder presented poorly bonded,

This article is an invited paper selected from presentations at the 2008 International Thermal Spray Conference and has been expanded from the original presentation. It is simultaneously published in *Thermal Spray Crossing Borders, Proceedings of the 2008 International Thermal Spray Conference*, Maastricht, The Netherlands, June 2-4, 2008, Basil R. Marple, Margaret M. Hyland, Yuk-Chiu Lau, Chang-Jiu Li, Rogerio S. Lima, and Ghislain Montavon, Ed., ASM International, Materials Park, OH, 2008.

Guan-Jun Yang, Chang-Jiu Li, Shi-Jun Zhang, and Cheng-Xin Li, State Key Laboratory for Mechanical Behavior of Materials, School of Materials Science and Engineering, Xi'an Jiaotong University, Xi'an, Shaanxi 710049, P.R. China. Contact e-mail: ygj@mail.xjtu.edu.cn.

cracked carbides and a coarse level of inhomogeneity (Ref 24). The high-temperature erosion of the HVOF sprayed $\text{Cr}_3\text{C}_2\text{-NiCr}$ coating by the erosive particles at relatively high velocity of more than 30 m/s was extensively reported (Ref 8-10), and the spray powder in the work was blended powder with NiCr alloy powder and Cr_3C_2 carbide powder. However, the high-temperature erosion of the coatings deposited with sinter-crushed powder is less well known.

The objective of this paper was to investigate the high-temperature erosion behavior of HVOF sprayed $\text{Cr}_3\text{C}_2\text{-NiCr}$ coatings deposited with sinter-crushed powder and compare that with the typical mild steel for boiler tubes.

2. Experimental Procedures

2.1 Materials

A sinter-crushed $\text{Cr}_3\text{C}_2\text{-25%NiCr}$ powder (Langli, Luoyang, China) was employed for HVOF spraying. The powder size ranged from 30 to 37.5 μm . A mild steel, which is often used to fabricate boiler tubes, was used as a substrate for the deposition of $\text{Cr}_3\text{C}_2\text{-NiCr}$ coating. The composition of the mild steel is shown in Table 1. The bare steel was also subjected to the erosion test for comparison.

2.2 Deposition of the Coating

$\text{Cr}_3\text{C}_2\text{-NiCr}$ coatings were deposited with a CH-2000 HVOF spray system (Xi'an Jiaotong University), the detailed description of which was given elsewhere (Ref 25). The system is operated using propane and oxygen to generate supersonic flame. Propane was used as fuel gas and operated at a pressure of 0.4 MPa and a flow of 1300 L/h. Oxygen was operated at a pressure of 0.55 MPa and a flow of 13,000 L/h. Nitrogen gas was used as a powder feed gas. The spray distance was 180 mm.

2.3 Characterization of the Coating

The topographic morphology and cross-sectional microstructures of the coating and the mild steel were examined by scanning electron microscopy (SEM) (Quanta 200, FEI, the Netherlands). Erosion of the coating and the mild steel was tested using the experiment setup as shown in Fig. 1. Alumina grit with a nominal size of 250 μm was employed as the erodent. The feed rate of erodent was 60 g/min. The erosive particles were accelerated to a velocity of 12 m/s by a modified HVOF spray torch. The

impact angles during test were fixed at 30° and 90°, respectively. The temperature of the testpieces including the coating and the mild steel plate during erosion test was set to 300, 500, 600, 700, and 800 °C, respectively. To eliminate the effect of surface conditions, all testpieces were polished before the erosion test. The erosion rate of the coating and the mild steel was evaluated by the weight loss divided by the weight of erosive particles. Under each test condition, three testpieces were used and the erosion rate was the average of three tests.

3. Results

3.1 Microstructure of the HVOF Sprayed $\text{Cr}_3\text{C}_2\text{-25%NiCr}$ Coating

Figure 2 shows the cross-sectional microstructure of the HVOF sprayed $\text{Cr}_3\text{C}_2\text{-NiCr}$ coating. The coating thickness was about 600 μm . The microstructure at a higher magnification shown in Fig. 2(b) revealed that the carbide particle size was several micrometers. The carbide particles were uniformly distributed in the coating. However, some pores were observed on the microstructure. The pores may have resulted from the pulling out of weakly bonded particles during the sample polishing process. It was found from Fig. 2 that the coating was well adhered to the substrate.

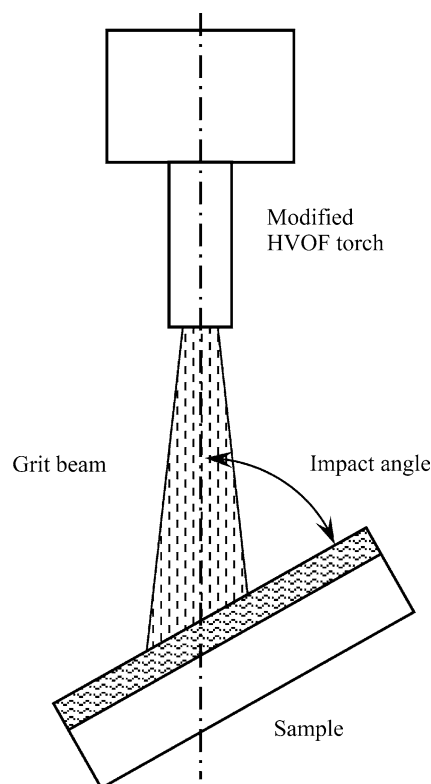


Fig. 1 Experimental setup for the high-temperature erosion test

Table 1 Composition of the mild steel for boiler tube

Element	Content, %
C	0.17-0.24
Si	0.17-0.37
Mn	0.35-0.65
S	≤0.035
P	≤0.035

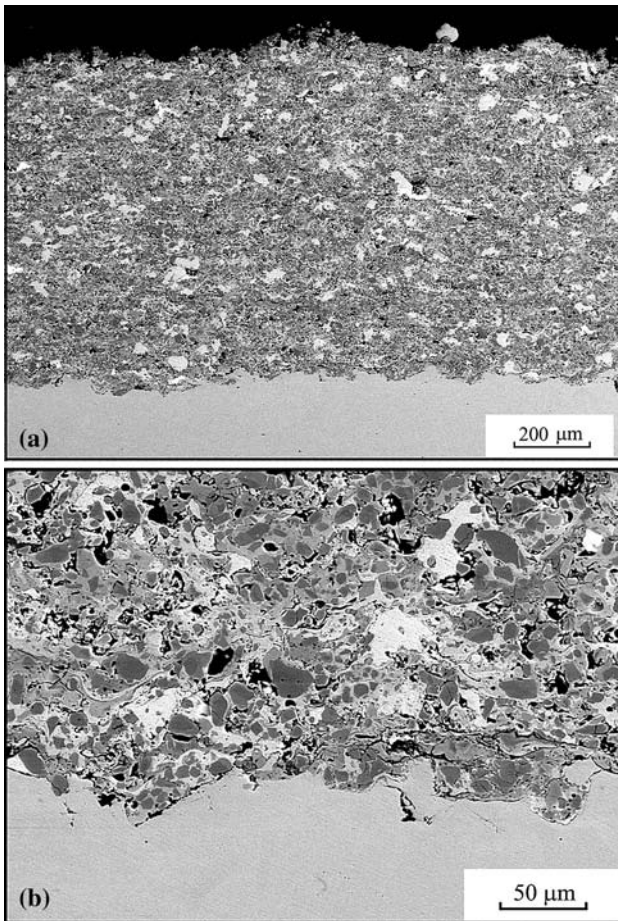


Fig. 2 Cross-section microstructure of the HVOF sprayed $\text{Cr}_3\text{C}_2\text{-NiCr}$ coating. (a) Low magnification. (b) High magnification

3.2 Erosion of the Coating and Mild Steel

Figure 3 shows the effect of sample temperature on the erosion rate of the mild steel. The erosion rate was significantly increased with the increase of the temperature at the impacting angles of both 30° and 90° . The erosion rate at 30° was 0.2 mg/g at a temperature of 300°C . The erosion rate at 800°C became more than four times higher than that at 300°C . At the impact angle of 90° , the erosion rate at 800°C was nearly seven times higher than that at 300°C . According to the erosion theory of ductile metallic materials, the erosion rate of metals becomes the maximum at impact angle range from about 15 to 20° (Ref 26). It will decrease with the increase of impact angle. It is clear that the present test results at the temperatures lower than 300°C follow the classical theory. However, it is clearly observed that with the increase of test temperature the relative erosion rate at 90° with respect to that at 30° becomes large. This is possibly attributed to poor oxidation resistance of the mild steel.

Figure 4 shows the effect of coating temperature on the erosion rate of the $\text{Cr}_3\text{C}_2\text{-NiCr}$ coating. The effect was very different from that for the mild steel. This is possibly

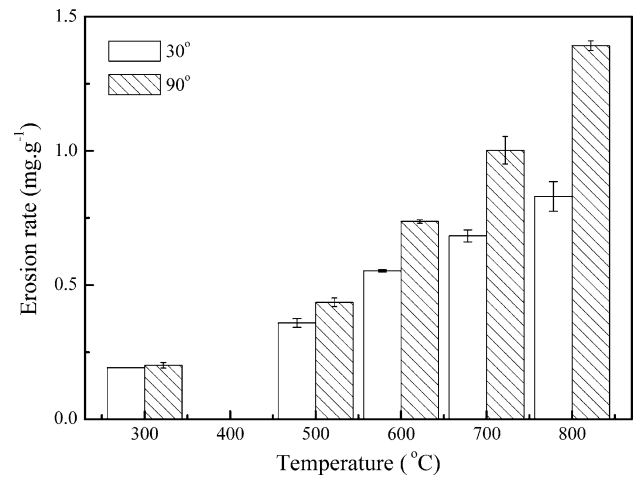


Fig. 3 Effect of erosion temperature on the erosion rate of mild steel

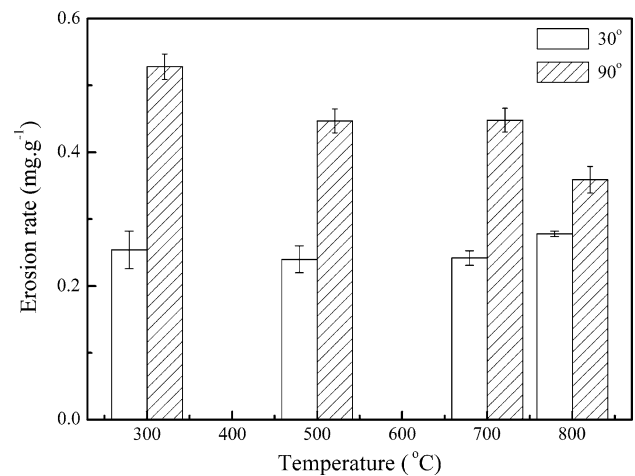


Fig. 4 Effect of erosion temperature on the erosion rate of the HVOF sprayed $\text{Cr}_3\text{C}_2\text{-NiCr}$ coating

attributed to the difference in the change of oxidation resistance of the $\text{Cr}_3\text{C}_2\text{-NiCr}$ coating from the mild steel with the increase of temperature. The erosion rate at 30° was 0.25 mg/g and independent of coating temperature in the range from 300 to 800°C . The erosion rate at 90° slightly decreased with the increase of the test temperature. Moreover, at a temperature of 300°C , the erosion rate of the coating at 90° was two times that at 30° . However, at 800°C , the erosion rate at 90° became comparable to that at 30° .

4. Discussion

Table 2 shows the erosion rate of the mild steel relative to that of the HVOF sprayed $\text{Cr}_3\text{C}_2\text{-NiCr}$ coating as a function of test temperature. It can be clearly seen that the relative erosion resistance of the coating increases with the

Table 2 Comparison of the erosion rate of the coating and the mild steel

Test temperature, °C	$Y_{\text{steel}}/Y_{\text{coating}}$	
	At 30°	At 90°
300	0.39	0.77
500	1.0	1.5
700	2.2	2.9
800	3.8	3.0

increase of test temperature. These results indicate that the coating exhibits a higher relative erosion resistance at higher test temperature. Although the relative erosion resistance of the coating at a test temperature of 300 °C is only 0.39-0.77 at the impact angles of 30° and 90°, respectively, it becomes larger than one at test temperatures higher than 500 °C. The relative wear resistance at 800 °C reaches to 3.8 and 3.0 at the impact angles of 30° and 90°, respectively.

It was evidently found that the erosion rate of the HVOF sprayed $\text{Cr}_3\text{C}_2\text{-NiCr}$ coating decreases with the increase of test temperature at an impact angle of 90°. This may be attributed to the composite characteristics of the coating. For ductile materials such as mild steel, the increase of test temperature leads to a decrease of hardness and therefore results in a significant decrease in erosion resistance. For the coating, the high content of hard carbide particles enables the coating to maintain a comparably high hardness even at high temperature. Furthermore, the apparent ductility of the coating is improved by the enhanced ductility of the NiCr alloy matrix at high temperature. When the coating is impacted by the erosive particles, the good ductility of the matrix allows the impacted local area of the coating to deform to prevent the surging of the highly localized stress that may result in cracking of the coating. Therefore, the erosion rate of the HVOF sprayed $\text{Cr}_3\text{C}_2\text{-NiCr}$ coating decreases with the increase of erosion temperature.

Figure 5 shows the topographical morphologies of the mild steel and the HVOF sprayed $\text{Cr}_3\text{C}_2\text{-NiCr}$ coating after erosion test at an impact angle of 30° and a temperature of 800 °C. It can be clearly seen from Fig. 5(a) that there are large ploughs in a width of tens of micrometers on the worn surface of the mild steel. This is attributed to a typical ductile erosion mechanism of the mild steel against alumina erosive particles. Small ploughs were also observed in the surface of the coating shown in Fig. 5(b). The width of these small ploughs is <2-5 μm . Therefore, the ploughs on the coating surface are much smaller than those on the mild steel surface. When the erosive particles impact on the coating surface at a low angle, the edge of an erosive particle will plough the surface. On account of the existence of hard carbide particles in the coating, only a small plough can be formed on the coating surface.

Figure 6 shows the cross-sectional morphology of the HVOF sprayed $\text{Cr}_3\text{C}_2\text{-NiCr}$ coating after erosion test at an impact angle of 30° and a temperature of 800 °C. A large

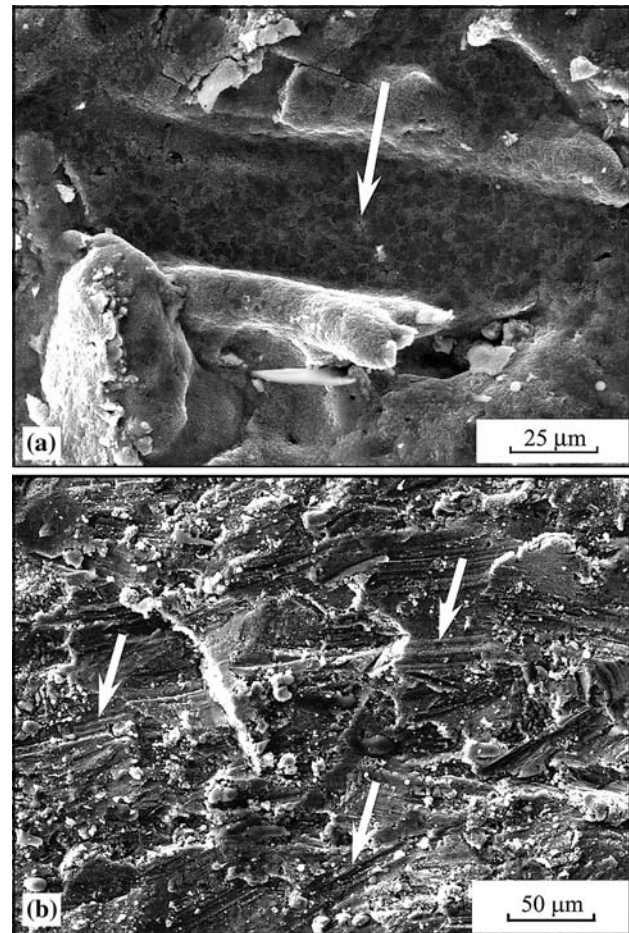


Fig. 5 Topographical morphology of the mild steel (a) and the HVOF sprayed $\text{Cr}_3\text{C}_2\text{-NiCr}$ coating (b) after erosion test at impact angle of 30° and temperature of 800 °C

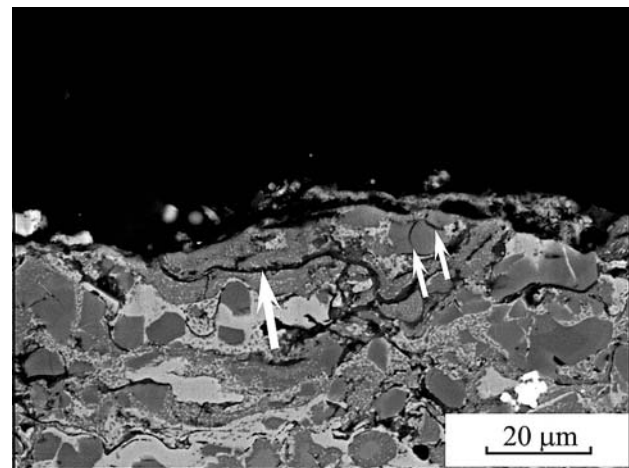


Fig. 6 Cross-section microstructure of the HVOF sprayed $\text{Cr}_3\text{C}_2\text{-NiCr}$ coating after erosion test at impact angle of 30° and temperature of 800 °C

crack marked with a large white arrow can be clearly observed near the coating surface. This is attributed to the impact of the erosion particles on the coating surface.

HVOF sprayed $\text{Cr}_3\text{C}_2\text{-NiCr}$ coatings are composed of splats, which are formed through spreading of solid-liquid particles with a NiCr matrix in molten state and Cr_3C_2 particles in solid state (Ref 17, 18). The adjacent two splats are bonded partially, and significant nonbonded area exists between the two splats (Ref 14, 17, 18). The partial bonding between splats was also supported by the fact that the cohesive strength of the HVOF sprayed $\text{Cr}_3\text{C}_2\text{-NiCr}$ coating was measured as 72 MPa (ASTM C 633-79), which is much less than the strength of the bulk cermet. The nonbonded area will act as a precrack, which propagates under the impact of erosive particles on the coating surface. Consequently, before the splat is completely ploughed by erosive particles, the crack propagation originating from the nonbonded interface area may lead to the flaking of one splat or several splats. In addition, cracks in carbide particles marked with two small white arrows are also observed in Fig. 6. The small carbides resulted from the cracking of the original large carbide particles. The new surface of small carbides was in the form of free surface, which was produced by the cracking of carbide particles. Therefore, these small particles were held less by the NiCr matrix. These particles are easily eroded off by the impact of erosion particles. Therefore, such cracking may also promote the erosion of the coating by removal of carbides by impact.

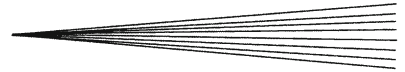
Although there are three mechanisms that cause the mass loss of the coating under erosive wear, splat flaking will be dominant over carbide cracking and ploughing. Therefore, the erosive resistance of the HVOF sprayed $\text{Cr}_3\text{C}_2\text{-NiCr}$ coating will predominantly depend on the extent of splat flaking. The results suggest that the erosion performance of the HVOF sprayed $\text{Cr}_3\text{C}_2\text{-NiCr}$ coating is controlled by the cohesion between splats in the coating and can be further enhanced by improving splat cohesion.

5. Conclusions

The erosion performance of the HVOF sprayed $\text{Cr}_3\text{C}_2\text{-NiCr}$ coating and a mild steel at temperatures from 300 to 800 °C was investigated using alumina grit as erodent. Results showed that the erosion rate of the mild steel increased with the increase of the test temperature at the erosion angles of both 30° and 90°. The erosion rate of the mild steel at 800 °C was four times higher than that at 300 °C at an erosion angle of 30°. However, the erosion rate of the HVOF sprayed $\text{Cr}_3\text{C}_2\text{-NiCr}$ coating at an erosion angle of 30° was not influenced by the test temperature in the range of 300-800 °C. It was found that the erosion resistance of HVOF sprayed $\text{Cr}_3\text{C}_2\text{-NiCr}$ coating was more than three times higher than that of the mild steel at 700-800 °C. The mass loss of the coating was attributed to splat flaking and ploughing on the surface. The results suggest that the erosion performance of the HVOF sprayed $\text{Cr}_3\text{C}_2\text{-NiCr}$ coating was controlled by the cohesion between splats in the coating and could be further enhanced by improving splat cohesion.

References

1. A. Gungor and N. Eskin, Two-Dimensional Coal Combustion Modeling of CFB, *Int. J. Therm. Sci.*, 2008, **47**, p 157-174
2. V.H. Hidalgo, F.J.B. Varela, A.C. Menendez, and S.P. Martinez, A Comparative Study of High-Temperature Erosion Wear of Plasma Sprayed NiCrBSiFe and WC-NiCrBSiFe Coatings under Simulated Coal-Fired Boiler Conditions, *Tribol. Int.*, 2001, **34**, p 161-169
3. V. Kain, K. Chandra, and B.P. Sharma, Failure of Carbon Steel Tubes in a Fluidized Bed Combustor, *Eng. Failure Anal.*, 2008, **15**, p 182-187
4. C. Yang and X. Gou, Dynamic Modeling and Simulation of a 410 t/h Pyroflow CFB Boiler, *Comp. Chem. Eng.*, 2006, **31**, p 21-31
5. J.S. Leszczynski, Z. Bis, and W. Gajewski, Evaluation of Structure and Particle Velocity Distribution in Circulating Fluidised Beds, *Powder Technol.*, 2002, **128**, p 22-35
6. M. Sawa and J. Oohori, Application of Thermal Spraying Technology at Steelworks, *Thermal Spraying: Current Status and Future Trends*, A. Ohmori, Ed., May 22-26 1995 (Kobe, Japan), High Temperature Society of Japan, 1995, 37 p
7. Y. Fukuda and M. Kumon, Application of High Velocity Flame Spraying for the Heat Exchanger Tubes in Coal Fired Boilers, *Thermal Spraying: Current Status and Future Trends*, A. Ohmori, Ed., May 22-26 1995 (Kobe, Japan), High Temperature Society of Japan, 1995, 107 p
8. B.Q. Wang, Chromium-Titanium Carbide Cermet Coating for Elevated Temperature Erosion Protection in Fluidized Bed Combustion Boilers, *Wear*, 1999, **225-229**, p 502-509
9. B.-Q. Wang and A. Verstak, Elevated Temperature Erosion of HVOF $\text{Cr}_3\text{C}_2/\text{TiC-NiCrMo}$ Cermet Coating, *Wear*, 1999, **233-235**, p 342-351
10. K.J. Stein, B.S. Schorr, and A.R. Marder, Erosion of Thermal Spray MCr- Cr_3C_2 Cermet Coatings, *Wear*, 1999, **224**, p 153-159
11. S.J. Matthews, B.J. James, and M.M. Hyland, Microstructural Influence on Erosion Behaviour of Thermal Spray Coatings, *Mater. Charact.*, 2007, **58**, p 59-64
12. I. Hussainova, Some Aspects of Solid Particle Erosion of Cermets, *Tribol. Int.*, 2001, **34**, p 89-93
13. J. Vicenzi, D.L. Villanova, M.D. Lima, A.S. Takimi, C.M. Marques, and C.P. Bergmann, HVOF-Coatings Against High Temperature Erosion (300 °C) by Coal Fly Ash in Thermoelectric Power Plant, *Mater. Des.*, 2006, **27**, p 236-242
14. G.-C. Ji, C.-J. Li, Y.-Y. Wang, and W.-Y. Li, Erosion Performance of HVOF-Sprayed $\text{Cr}_3\text{C}_2\text{-NiCr}$ Coatings, *J. Therm. Spray Technol.*, 2007, **16**(4), p 557-565
15. M. Factor and I. Roman, Use of Microhardness as a Simple Means of Estimating Relative Wear Resistance of Carbide Thermal Spray Coatings: Part 2. Wear Resistance of Cemented Carbide Coatings, *J. Therm. Spray Technol.*, 2002, **11**(4), p 482-495
16. J.K.N. Murthy and B. Venkataraman, Abrasive Wear Behaviour of WC-CoCr and $\text{Cr}_3\text{C}_2\text{-20(NiCr)}$ Deposited by HVOF and Detonation Spray Processes, *Surf. Coat. Technol.*, 2006, **200**, p 2642-2652
17. C.-J. Li, Y.-Y. Wang, G.-J. Yang, A. Ohmori, and K.A. Khor, Effect of Solid Carbide Particle Size on Deposition Behavior, Microstructure and Wear Performance of HVOF Cermet Coatings, *Mater. Sci. Technol.*, 2004, **20**, p 1087-1096
18. G.-C. Ji, C.-J. Li, and Y.-Y. Wang, Microstructural Characterization and Abrasive Wear Performance of HVOF Sprayed $\text{Cr}_3\text{C}_2\text{-NiCr}$ Coating, *Surf. Coat. Technol.*, 2006, **200**, p 6749-6757
19. R. Schwetzkke and H. Kreye, Microstructure and Properties of Tungsten Carbide Coatings Sprayed with Various High-Velocity Oxygen Fuel Spray Systems, *J. Therm. Spray Technol.*, 1999, **8**(3), p 433-439
20. J. He and E.J. Lavernia, Precipitation Phenomenon in Nanostructured $\text{Cr}_3\text{C}_2\text{-NiCr}$ Coatings, *Mater. Sci. Eng. A*, 2001, **301**, p 69-79
21. M. Roy, A. Pauschitz, J. Bernardi, T. Koch, and F. Franek, Microstructure and Mechanical Properties of HVOF Sprayed Nanocrystalline $\text{Cr}_3\text{C}_2\text{-25(Ni20Cr)}$ Coating, *J. Therm. Spray Technol.*, 2006, **15**(3), p 372-381



22. S. Matthews, M. Hyland, and B. James, Microhardness Variation in Relation to Carbide Development in Heat Treated $\text{Cr}_3\text{C}_2\text{-NiCr}$ Thermal Spray Coatings, *Acta Mater.*, 2003, **51**, p 4267-4277
23. S. Matthews, M. Hyland, and B. James, Long-Term Carbide Development in High-Velocity Oxygen Fuel/High-Velocity Air Fuel $\text{Cr}_3\text{C}_2\text{-NiCr}$ Coatings Heat Treated at 900 °C, *J. Therm. Spray Technol.*, 2004, **13**(4), p 526-536
24. S. Wirojanupatump, P.H. Shipway, and D.G. McCartney, The Influence of HVOF Powder Feedstock Characteristics on the Abrasive Wear Behaviour of $\text{Cr}_x\text{C}_y\text{-NiCr}$ Coatings, *Wear*, 2001, **249**, p 829-837
25. C.-J. Li, H. Yang, and H. Li, Effect of Gas Conditions on HVOF Flame and Properties of WC-Co Coatings, *Mater. Manuf. Process.*, 1999, **14**, p 383-395
26. P.A. Engel, *Impact Wear of Materials*. Elsevier, Amsterdam, 1976